Proceedings of the 4th IEEE Int. Conf. on
Nano/Micro Engineered and Molecular Systems
January 5-8, 2009, Shenzhen, China

Effect of Al Thickness on the Al Induced Low Temperature Poly-Si Film Crystallization Process

Hsiao-Yeh Chu[1,*], Ming-Hang Weng[2], Ru-Yuan Yang[3], Chien-Wei Huang[4], Chia-Hsing Li[1]

[1] *Micro and Precision Manufacturing Center & Mechanical Engineering Department, Kun Shan University. Taiwan, R.O.C.*
[2] *Metal Industries Research & Development Centre. Taiwan, R.O.C.*
[3] *Department of Materials Engineering, National Ping Tung University of Science & Technology. Taiwan, R.O.C.*
[4] *Department of Mechanical and Electro-Mechanical Engineering, National Sun Yat-sen University. Taiwan, R.O.C.*

Abstract — **In our previous study, we fabricates large grain low temperature poly-crystalline silicon film by aluminum induced crystallization (AIC) method. The fabrication process is to deposite aluminum layer on top of the a-Si:H film deposited by plasma enhanced chemical vapor deposition (PECVD) [1]. In this paper, we discussed more about the effect of different aluminum thickness of the AIC process. Five kinds of specimens with different aluminum thickness of, 10, 20, 40, 80, and 160 nm, respectively; are fabricated and tested. The annealing temperature is set at 350°C and 30 min in the annealing stage. The crystallinity of the annealed silicon film is discussed in this paper. XRD and Raman spectra analysis are used to identify the crystallinity of specimens made under different aluminum thicknesses. Raman results show that a-Si film will be crystallized if the Al film thickness is over 40 nm aluminum thickness. The crystallinity volume fraction calculated is about 45~90%. The I-V characteristic is tested to see the magnitude of leakage current of poly silicon film made in our study.**

Keywords —***low temperature polycrystalline silicon, film thickness, aluminum induced crystallization, metal induced crystallization***

I. INTRODUCTION

Low temperature poly silicon (LTPS) has been studied for thin film solar cell, TFT-LCD, photodetector and other optoelectric-related applications [2, 3]. The carrier mobility of a poly-Si thin film is 10 to 100 times larger than that of an a-Si:H film [4], poly silicon film is one of the most important way to be applied to the solar cell panel in order to meeting the insufficient quantity of bulk Si wafer need.

Three categories of methods are commonly used to fabricate poly-Si film on glass: Catalytic-CVD method [5], excimer laser annealing (ELA) method [6, 7] and metal induced crystallization (MIC) method [8-12]. AIC is one of the MIC methods. It can be applied to glass substrate at a temperature lower than 500°C [13]. AIC can induce low-temperature crystallization below the eutectic temperature (577°C) of Al and Si. It is possible to achieve a film with large lateral grain size compared to the film thickness. The lateral grain size of the poly-Si layer fabricated by the AIC method is about several μm.

In this study, we fabricate AIC specimens with different Al film thickness in order to see the minimum Al film thickness that can induce Si crystallization. The crystallinity of the poly silicon film is discussed by XRD and Raman spectra results. The crystalline volume fraction is calculated from those results. The current densities of the specimens are tested by the I-V tester.

II. EXPERIMENTAL

It has been proven that the a-Si/Al method (Al film is deposited on top of a-Si film) can yield a lower AIC reaction temperature than the Al/a-Si method (Al film is deposited on bottom of a-Si film) [9]. Therefore, we used the a-Si/Al method to fabricate the Al induced low temperature poly-Si film in our study.

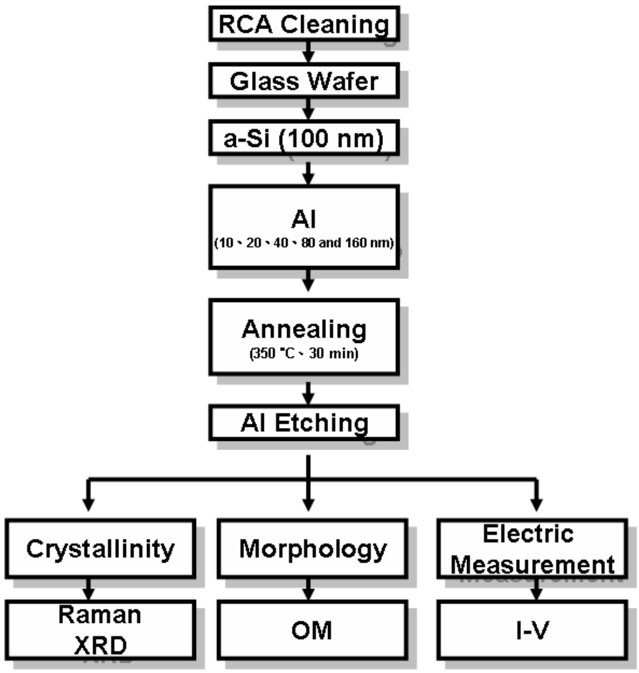

Figure 1. Process flow of the AIC method

Fig.1 shows the process flow of the experiment in our study. The substrate used in our study was Eagle2000 glass. The glass cleaning process was applied before film deposition. Table 1 shows the details of the glass cleaning process in our study. Amorphous silicon film of 100 nm thick was deposited on top of the substrate by plasma enhanced chemical vapor deposition (PECVD) after glass cleaning process. The power, chamber pressure, substrate temperature, and gas flow rate were: 100 W, 1 torr, 300°C, and 1200 sccm (SiH_4 30 sccm/N_2 1170 sccm), respectively. The deposition rate was about 1 nm/s. After the deposition of a-Si film, the samples were removed from the PECVD system, and then transferred to a sputter for the deposition of different thickness (10, 20, 40, 80, or 160 nm) of aluminum film. The process pressure is 5×10^{-3} torr. The deposition rate is about 1 nm/s. The substrate temperature is about 25°C. The sputtering power is 1000 W. When the aluminum deposition process was finished, the specimen was cut into small pieces and annealed at 350°C for 30 minutes in an N_2 environment with ramp-up time period of 1 hour. These small pieces of specimens were all under vacuum environment during ramp-up time period of annealing process. Nitrogen flowed into the furnace when the chamber temperature reached to 350°C. The specimens were then kept furnace cooling after 30 minutes of annealing. The remaining Al was then removed by wet selective etching for 60 seconds. The etchant consists of 70% of phosphoric acid, 20% of nitric acid and 10% of acetic acid. The temperature of the etching solution was 70°C.

TABLE I. DETAIL OF GLASS CLEANING PROCESS

Cleaning process	Method	Working temperature (°C)	Process time (s)
1. Acetone	Ultrasonic bath	Clean Room temperature	600
2. DI water	Ultrasonic bath	Clean Room temperature	600
3. Gas drying	N_2 gun	Clean Room temperature	30
4. Baking	Hot plate	90	600

III. RESULTS AND DISCUSSION

Fig.2 shows the surfacial images results of the optical microscope (OM) of the poly-Si film after annealing with different aluminum film thickness. Large sizes of poly silicon grain are observed when the aluminum film thickness is greater than 40 nm. There is no poly silicon grain found in the cases of 10 and 20 nm aluminum film thicknesses. It is therefore evident from the optical microscope observation that if the aluminum film thickness is less than 20 nm, there will be no poly silicon being crystalized for the a-Si/Al AIC method. The result of Raman spectra analysis and XRD results on the crystallinity of poly silicon will be used as the evidence of the above discussion.

Fig.3 shows the Raman spectra of poly-Si film after annealing with different aluminum film thicknesses. If the Al film thickness is 10 nm, there is no obvious peak shown. If the Al film thickness is 20 nm, there is a peak with its strongest intensity located at about 480 cm^{-1}. It shows that the silicon film is still amorphous in this case. As the Al film thickness is over 20 nm, there is a peak shown in each case. The peak intensity moves toward 520 cm^{-1} as the aluminum film thickness increases from 40 to 160 nm. The Raman shift of the peak intensity which is closer and closer to 520 cm^{-1} with the increase of aluminum film thickness means that the crystallization of amorphous silicon is better and better since the Raman shift of the crystallized silicon is located at about 521 cm^{-1}. It coincides with the OM observation discussed in Fig.2.

Fig.4 shows the XRD spectra of poly-Si films after annealing with different aluminum film thickness. The peak intensities located at 2θ=28°, 47°, and 56° indicate the crystalization orientations of Si(111), Si(200), and Si(311), respectively, from the comparison of JCPDS Card. Three peaks, Si (111), (220), and (311), exist in the cases of 40, 80, and 120 nm aluminum film thickness as shown in Fig.4. This further coincides with our OM and Raman results. Therefore, Poly-Si is successfully induced in the cases of 40, 80, and 120 nm aluminum film thickness.

Fig.5 shows the leakage current densities variation of specimens versus bias voltage under five different aluminum film thicknesses. The leakage current density is as low as 10^{-12} A/cm^2 in the case of 10 nm aluminum film thickness. If the aluminum film thickness increases from 10 to 20 nm, the leakage current density abruptly increases from 10^{-12} A/cm^2 to the order of 10^{-7} A/cm^2. The leakage current density will further increase from 10^{-7} to the 10^{-5} A/cm^2 with the increasing of aluminum film thickness from 40 to 160 nm. It shows that the leakage current density increases with the increase of aluminum film thickness, but the rate of increasing will be slower and slower although the aluminum film thickness increases exponentially.

IV. CONCLUSION

This paper reports the effect of aluminum film thickness on the surface morphology, crystallinity and leackage current density for the a-Si/Al AIC method. There is no poly silicon crystallization in the cases of 10 and 20 nm aluminum film thicknesses. The crystallization becomes better and better with the increase of aluminum film thickness from the results of both Raman spectra and XRD analyses. The maximum leakage current density also increases with the increase of aluminum filn thickness. The maximum leakage current density is about of the order of 10^{-5} A/cm^2 when the aluminum film thickness is over 80 nm.

ACKNOWLEDGMENT

We thank National Nano Device Laboratories for its support of specimens' fabrication and IV tests. We give thanks to National Ping Tung University of Science and Technology for its support of XRD measurements. We also give thanks to Ming Chang Shih in National University of Kaohsiung and Prof. Chien-Cheng Liu in Kun Shan University for their kind helps on the Raman measurements and annealing process conducted in his lab, respectively.

REFERENCES

[1] Hsiao Yeh Chu, Ming-Hang Weng, Ru-Yuan Yang, Chien-Wei Huang, and Chien-Cheng Liu, "Fabrication and Analysis of Nano-Aluminum-Induced Low-Temperature Polycrystalline Silicon Film", 2007 International Conference on Advanced Manufacture, Nov. 26-30, 2007, Tainan, Taiwan.

[2] Per I. Widenborg, Armin G. Aberle, "Hydrogen-induced dopant neutralization in p-type AIC poly-Si", Journal of Crystal Growth, vol 306, pp. 177-186, 2007

[3] M. Wang, Z. Meng, Y. Zohar and M. Wong," Metal-Induced Laterally Crystallized Polycrystalline Silicon for Integrated Sensor Applications", IEEE- Trans. Electron Devices vol. 48, no. 4, pp. 749-800.

[4] S W. Lee, Y C. Jeon, and S K. Joo, "Pd induced lateral crystallization of amorphous Si thin films," Appl. Phys. Lett., vol. 66, no. 13, pp. 27, March 1995.

[5] O. Ebil, R. Aparicio, S. Hazra, R. W. Birkmir, and E. Sutterb, "Deposition and structural characterization of poly-Si thin films on Al-coated glass substrates using hot-wire chemical vapor deposition," Thin Solid Films, vol. 430, pp. 120-124, 2003.

[6] H. Azuma, A. Takeuchi, T. Ito, H. Fukushima, T. Motohiro, M. Yamaguchi, "Pulsed KrF excimer laser annealing of silicon solar cell," Solar Energy Materials & Solar Cells, vol. 74, pp. 289-294, 2002.

[7] F. Zhang, X. Liu, G. Ni, Y. Du, "Controlled growth of high-quality poly-silicon thin films with huge grains on glass substrates using an excimer laser," Journal of Crystal Growth, vol. 260, pp. 102-108, 2004.

[8] L S. Hung, F W. Saris, S Q. Wang, and J W. Mayer, "Interactions of amorphous alloys with Si substrates and Al overlayers," J. Appl. Phys., vol. 59, no. 7, pp. 2416, 1986.

[9] M S. Haque, H A. Naseem, and W D. Brown, "Interaction of aluminum with hydrogenated amorphous silicon at low temperatures," J. Appl. Phys., vol. 75, no. 8, p. 3928, 1994.

[10] M S. Ashtikar and G L. Sharma, "Silicide mediated low temperature crystallization of hydrogenated amorphous silicon in contact with aluminum," J. Appl. Phys., vol. 78, no. 2, p. 913-918, 1995.

[11] H. Kim, G. Lee, D. Kim, and S H. Lee, "A study of polycrystalline silicon thin films as a seed layer in liquid phase epitaxy using aluminum-induced crystallization," Current Applied Physics, vol. 2, pp. 129-133, 2002.

[12] P I. Widenborg, and A G. Aberle, "Surface morphology of poly-Si films made by aluminium-induced crystallization on glass substrates," Journal of Crystal Growth, vol. 242, 270-282, 2002.

[13] H. Azuma, A. Takeuchi, T. Ito, H. Fukushim, T. Motohiro, M. Yamaguchi," Pulsed KrF excimer laser annealing of silicon solar cell", Solar Energy Materials & Solar Cells, Vol. 74, p. 289-294, 2002.

[14] S. Verrek, F.A. Sarott and Z. Iqbal, "Effect of Grain Boundaries on the Raman Spectra,Optival Absorption, and Elastic Light Scattering in Nanometer-Sized Crystalline Silicon" Physical Review B, Vol 36,pp. 3344-3350,1987

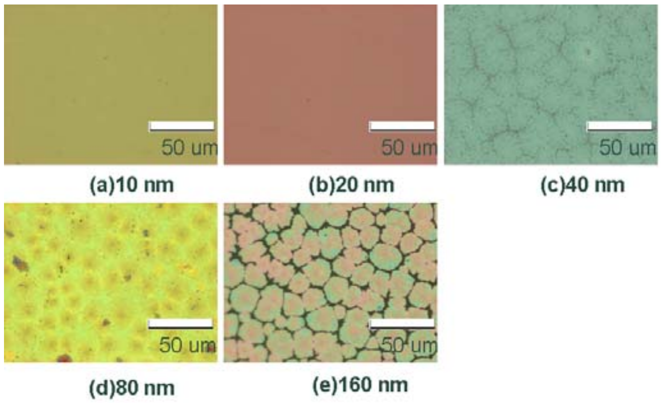

Figure 2. OM top view images of poly silicon films with different aluminum thickness of (a)10, (b)20, (c)40, (d)80, and (e)160 nm.

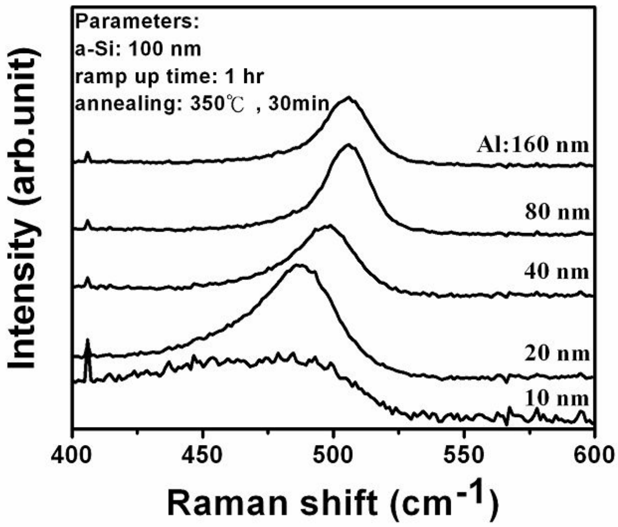

Figure 3. Raman spectra of poly silicon films with five different aluminum thicknesses.

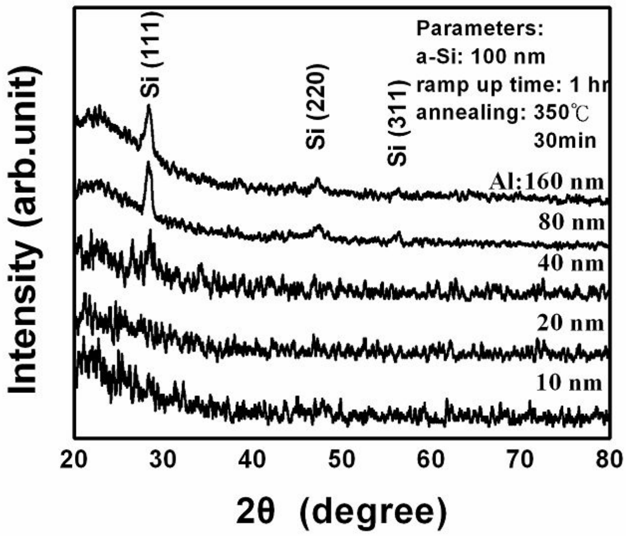

Figure 4. XRD spectra of poly silicon films with five different aluminum thicknesses.

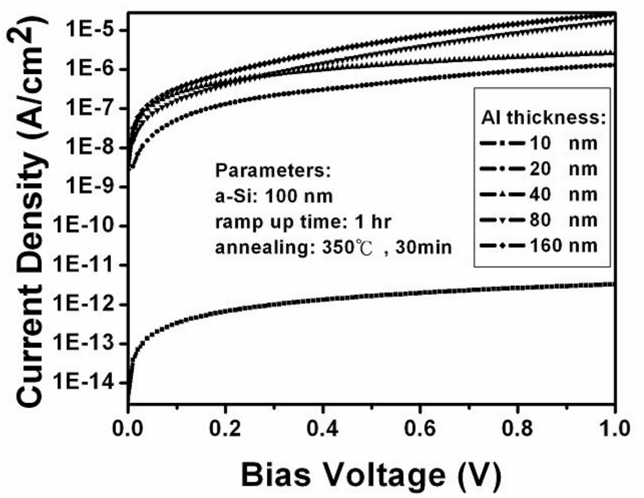

Figure 5. Leakage current density of specimens vs bias voltage under different aluminum thicknesses.